MHD avalanches in magnetized solar plasma

proliferation and heating in coronal arcades

Jack Reid[1]
James Threlfall,[2] Alan W. Hood[1]

[1]University of St Andrews
[2]Abertay University

30 June 2022

University of St Andrews | FOUNDED 1413

Motivation: solar coronal heating in multi-stranded loops

- Coronal heating problem: what mechanisms sustain hot coronal temperatures in the Sun's atmosphere?
- On larger scales, such a mechanism could cause bright flaring emission
- Coronal loops:
  - greatest concentrations of heating,
  - curved between footpoints anchored on the solar surface
  - appearing as bundles of fine, bright strands, tracing the magnetic field

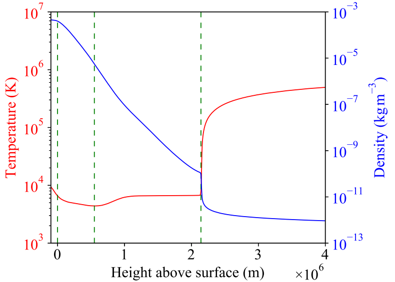

Temperature and density v. height.

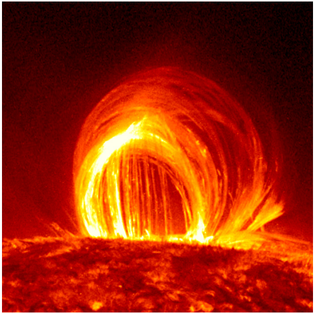

Observed coronal loop.

Self-organized criticality

- SOC: system in easily perturbed, critical, minimally stable state
  - e.g. adding one grain may leave a sand-pile unchanged, or could cause a flow down its side
- Avalanche: one small, local disturbance starts chain reaction of events
- Events collectively dissipate substantial energy

Favoured example of SOC state: sand-pile.

Chain reaction.

Self-organized criticality.

Proposition: MHD avalanches through ‘nanoflares’

- Self-organized criticality applied to the corona (Lu & Hamilton 1991)
- Corona is driven from below by photospheric granulation
- Eventually, a local instability occurs
- Chain reaction ensues, with like instabilities at neighbouring sites
- Coronal heating via cumulative energy release in small ‘nanoflare’ events
  - as proposed by the late Eugene Parker (Parker 1988)

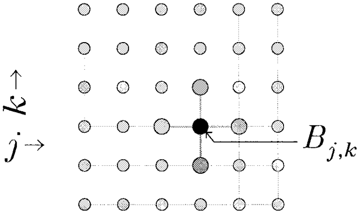

NANOFLARES AND THE SOLAR X-RAY CORONA[1]

E. N. PARKER

Enrico Fermi Institute and Departments of Physics and Astronomy, University of Chicago

Received 1987 October 12; accepted 1987 December 29

ABSTRACT

Observations of the Sun with high time and spatial resolution in UV and X-rays show that the emission from small isolated magnetic bipoles is intermittent and impulsive, while the steadier emission from larger bipoles appears as the sum of many individual impulses. We refer to the basic unit of impulsive energy release as a *nanoflare*. The observations suggest, then, that the active X-ray corona of the Sun is to be understood as a swarm of nanoflares.

This interpretation suggests that the X-ray corona is created by the dissipation at the many tangential discontinuities arising spontaneously in the bipolar fields of the active regions of the Sun as a consequence of random continuous motion of the footpoints of the field in the photospheric convection. The quantitative characteristics of the process are inferred from the observed coronal heat input.

Subject headings: hydromagnetics — Sun: corona — Sun: flares

Geometry of models of coronal loops: straight v. curved

Families of models of coronal loops

- Parker (1972)'s conventional model: straightened between two planes
  - topologically equivalent to curved, cylindrical loops
  - straightforward to study and model
- Truly, geometrically curved loops
  - closely resemble observable loops
  - more challenging to implement

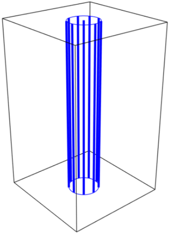

Straightened Parker model.

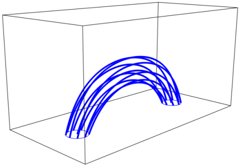

Truly curved.

Models of loops.

Model: curved magnetic field

- Initially potential arcade, mostly vertical near footpoints
- Changing polarity across inversion line (PIL; $y = 0$)
- Flux tubes extend in y; field decays with height z
- Resembling bipolar regions in active regions

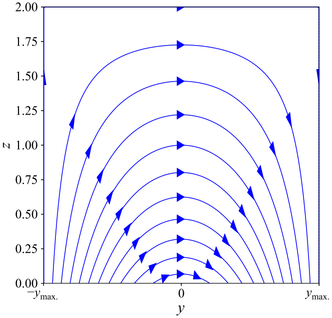

Field lines.

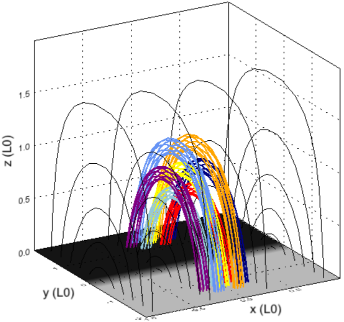

Curved field lines in component strands.

Initial, curved magnetic field in arcade.

Model: photospheric rotations

- Simple, vortical motions at footpoints
- Flux tubes formed out of ambient field
- Poynting flux injects energy, as magnetic field is twisted
- Energy accumulates in corona until critically unstable

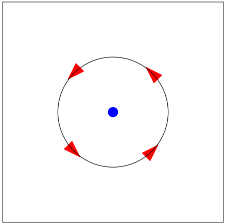

Rotation.

Driving imposed.

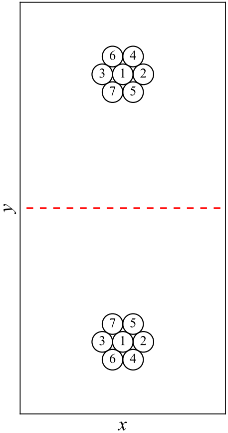

Arrangement on base.

Footpoints.

Methodology: numerical simulations

$$\frac{\mathrm{D}\rho}{\mathrm{D}t} = -\rho\left(\nabla\cdot\mathbf{v}\right)$$

$$\rho\frac{\mathrm{D}\mathbf{v}}{\mathrm{D}t} = -\nabla P + \mathbf{j}\times\mathbf{B} + \mathbf{F}_{\mathrm{visc.}}$$

$$\rho\frac{\mathrm{D}\varepsilon}{\mathrm{D}t} = -P\left(\nabla\cdot\mathbf{v}\right) + \frac{j^2}{\sigma} + Q_{\mathrm{visc.}}$$

$$\frac{\mathrm{D}\mathbf{B}}{\mathrm{D}t} = \left(\mathbf{B}\cdot\nabla\right)\mathbf{v} - \mathbf{B}\left(\nabla\cdot\mathbf{v}\right) - \nabla\times\left(\frac{1}{\sigma}\mathbf{j}\right)$$

$$P = \frac{\rho k_B T}{\mu_m}$$

- Three-dimensional numerical simulations solve MHD equations
- *Lare* (Arber et al. 2001) code
- Viscosities
  - Shock
  - Background
- Anomalous resistivity on strong currents

$$\zeta = \frac{|\mathbf{j}|}{|\mathbf{B}|}$$

$$\eta = \begin{cases} \eta_0 & \zeta > \zeta_{\mathrm{crit.}} \\ 0 & \zeta \le \zeta_{\mathrm{crit.}} \end{cases}$$

Build-up to instability

Fastest rotation in central flux tube ⇒ it attains greatest twist ⇒ first instability

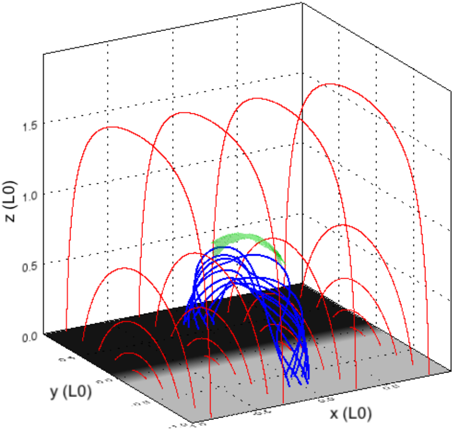

Field lines in twisted flux tube (blue), embedded within those of an arcade (red), producing a current sheet (green).

Onset of instability

Strong crescent of toroidal current causes resistivity and dissipation

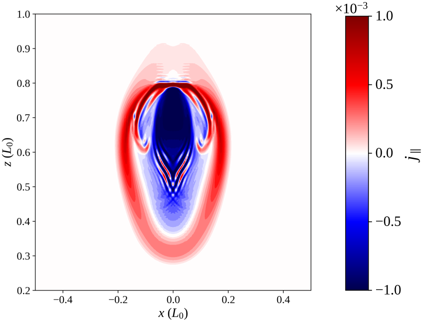

Toroidal current.

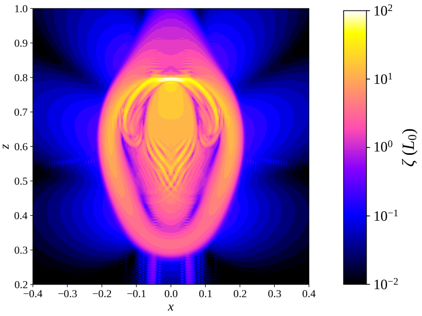

Critical resistive parameter ζ.

Cross-section at the apex (above PIL).

Nature of instability

- Does geometry affect instability?
- Kink mode
  - occurs in a twisted flux tube
  - deforms ('kinks')
- Twist Φ here reaches critical level in first flux tube (per Hood & Priest 1979)
- Phase angle of kink mode
  - Usually arbitrary
  - Here, invariably upwards

$\Rightarrow$ Modified, directed kink mode

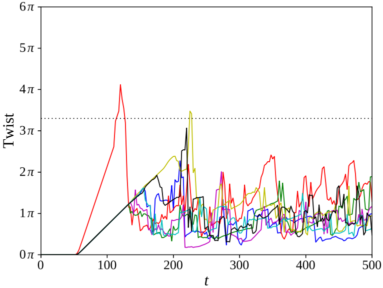

Twist in different flux tubes (different colours).

Indicator of instability.

$$\langle \Phi \rangle \approx 3.20\,\pi \qquad \Phi_{\text{crit.}} \approx 3.3\,\pi$$

Nature of instability

- Does geometry affect instability?
- Kink mode
  - occurs in a twisted flux tube
  - deforms (‘kinks’)
- Twist Φ here reaches critical level in first flux tube (per Hood & Priest 1979)
- Phase angle of kink mode
  - Usually arbitrary
  - Here, invariably upwards

  $\Rightarrow$ Modified, directed kink mode
- Torus instability also plausible, but less likely

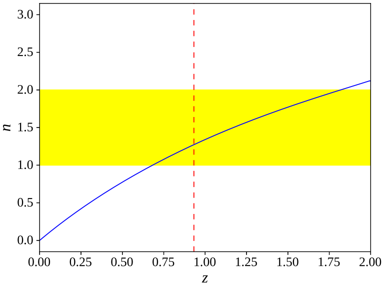

Torus decay index varying with height.

Indicator of instability.

$n \approx 1.5 \qquad n_{\text{crit.}} \approx 1.0\text{–}2.0$

Chain reaction: proliferation of avalanche

- Central flux tube first unstable
- Avalanche spreads via chain reaction
- Other tubes ‘nudged’ in turn
- Disruption spreads over very widespread area

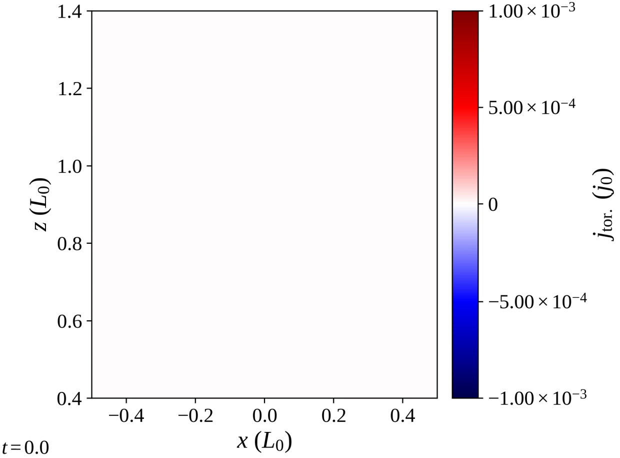

Toroidal current.

Heating: ‘nanoflares’

- Temporally, heating is impulsive and intermittent: Parker’s nanoflares
- Heating events convert magnetic energy into kinetic and thermal

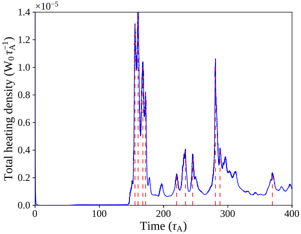

Total heating.

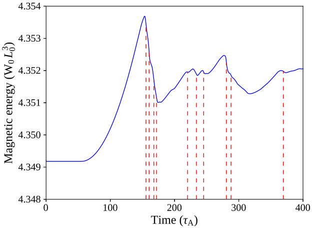

Magnetic energy.

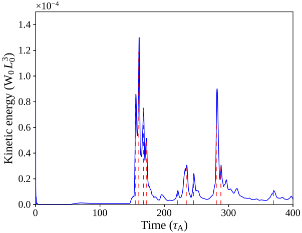

Kinetic energy.

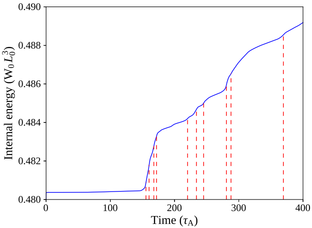

Internal energy.

Heating: evolution and composition

- MHD heating mechanisms:
  - shocks,
  - viscosity,
  - Ohmic heating
- Shock and viscous heating dominate

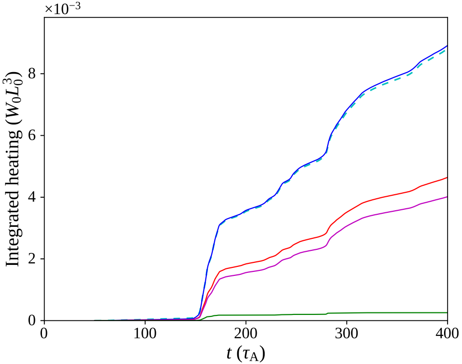

Contributions to increase in thermal energy (net, cyan).

Total heating in arcade.

Heating: evolution and composition

- MHD heating mechanisms:
  - shocks,
  - viscosity,
  - Ohmic heating
- Shock and viscous heating dominate
- Heating seems aperiodic

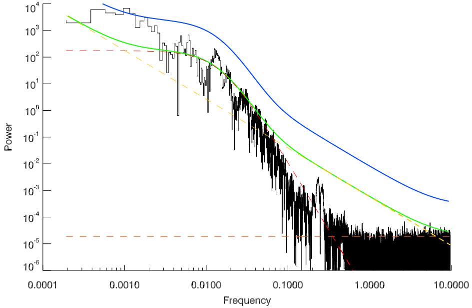

Fourier transform.

Total heating in arcade.

Heating: evolution and composition

- MHD heating mechanisms:
  - shocks,
  - viscosity,
  - Ohmic heating
- Shock and viscous heating dominate
- Heating seems aperiodic
- Consistently, about half of injected energy is dissipated

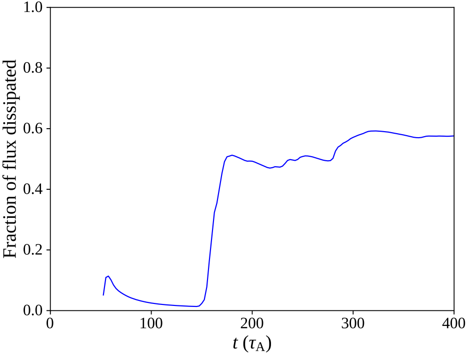

Cumulatively, as fraction of injected energy.

Total heating in arcade.

Contours of heating

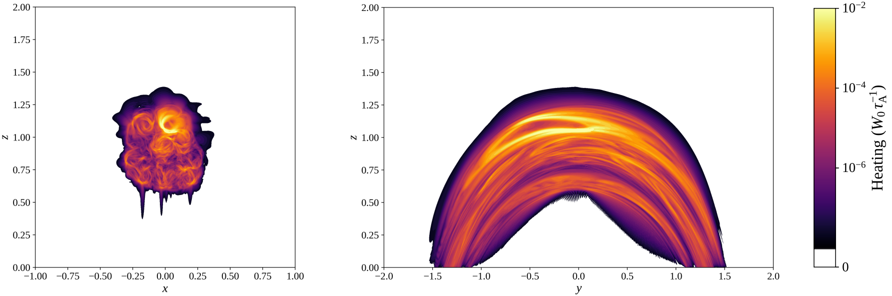

In cross-section at apex. *Along length of loop.*

Contours of total heating.

Current layers

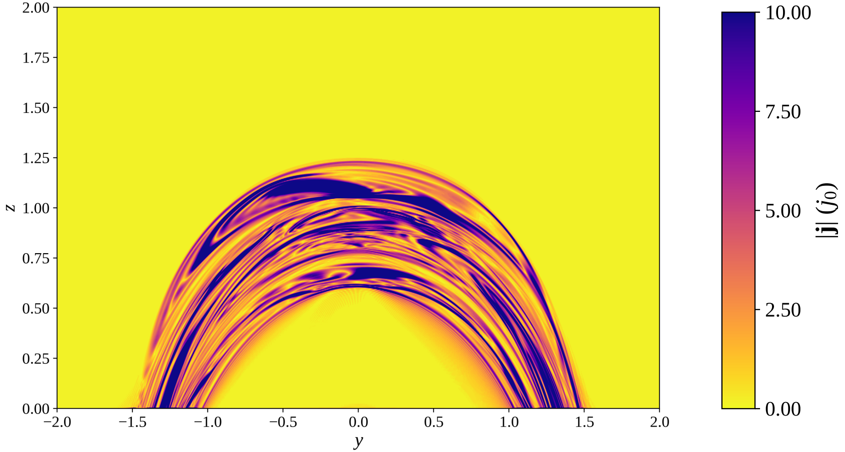

Contours of magnitude of current.

Discussion

Conclusions

- Avalanches viable in curved, as in straightened, models of flux tubes
- Nature of instability modified by geometry and curvature
- Heating:
  - highly time-dependent
  - predominantly from shocks and viscosity
  - spatially dispersed and localized

Future work

- What differences emerge from new geometry?
- Comparison of heating between models
- Self-consistent treatment of thermodynamic response in 3D MHD

References

- Arber, T. D. et al. (2001). ‘A Staggered Grid, Lagrangian-Eulerian Remap Code for 3-D MHD Simulations’. *J. Comput. Phys.* **171**(1), pp. 151–181.
- Hood, A. W. and Priest, E. R. (1979). ‘Kink Instability of Solar Coronal Loops as the Cause of Solar Flares’. *Sol. Phys.* **64**(2), pp. 303–321.
- Lu, Edward T. and Hamilton, Russell J. (1991). ‘Avalanches and the Distribution of Solar Flares’. *ApJ* **380**, pp. L89–L92.
- Parker, E. N. (1972). ‘Topological Dissipation and the Small-Scale Fields in Turbulent Gases’. *ApJ* **174**(4), pp. 499–510.
- – (1988). ‘Nanoflares and the Solar X-ray Corona’. *ApJ* **330**, pp. 474–479.